ACS OMEGA

http://pubs.acs.org/journal/acsodf

Article

Effect of Surface Modifications on Cellular Uptake of Gold Nanorods in Human Primary Cells and Established Cell Lines

Yuxiang Xiao, Wei Xu, Yoshihiro Komohara, Yukio Fujiwara, Hisaaki Hirose, Shiroh Futaki, and Takuro Niidome*

Cite This: *ACS Omega* 2020, 5, 32744−32752

Read Online

ACCESS | Metrics & More | Article Recommendations

ABSTRACT: Endocytosis is a cellular process in which substances are engulfed by the cellular membrane and budded off inside the cells to form vesicles. It plays key roles in controlling nutritional component uptake, immune responses, and other biological functions. A comprehensive understanding of endocytosis gives insights into such physiological functions and informs the design of medical nanodevices that need to enter cells. So far, endocytosis has been studied mostly using established cell lines. However, the established cell lines generally originate from cancer cells or are transformed from normal cells into immortalized cells. Therefore, primary cells may give us more reliable information about the endocytosis process of nanoparticles into cells. In this research, we studied the uptake of gold nanorods (AuNRs) with four different surface modifications (anionic/cationic polymers and anionic/cationic silica) by two kinds of primary cells (human monocyte-derived macrophages and human umbilical vein endothelial cells) and two kinds of established cell lines (HeLa cells and RAW 264.7 cells). We found that the surface properties of AuNRs affected their cellular uptake, and the cationic surface tended was advantageous for uptake, but it depended on the cell types. Control experiments using inhibitors of representative endocytosis pathways (macropinocytosis, clathrin-mediated endocytosis, and caveolae-mediated endocytosis) indicated that primary cells had a dominant uptake pathway for internalization of the AuNRs, whereas the established cell lines had multiple pathways. Our results provide us with novel insights into cellular uptake of AuNRs in that they depend not only on surface characters of the nanoparticles but also cell types, such as primary cells and established cell lines.

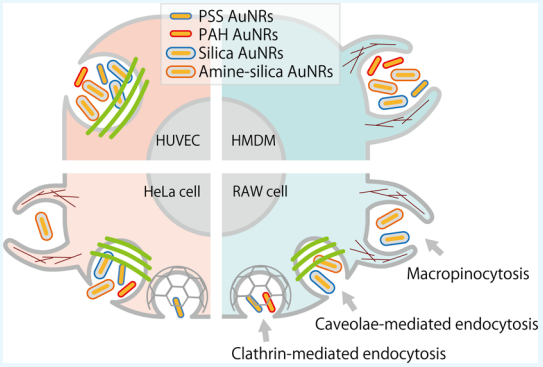

INTRODUCTION

Endocytosis is a cellular process, in which substances are engulfed by the cellular membrane and budded off inside of the cells to form vesicles, known as endosomes.[1,2] It is not only essential to take in nutritional components for cellular growth, immune responses, and other biological functions[3,4] but also an important infection mechanism for microorganisms.[5,6] Endocytosis is energy-dependent and categorized into macropinocytosis, clathrin-mediated endocytosis, caveolae-mediated endocytosis, and clathrin and caveolin-independent endocytosis.[7] All these varying endocytic processes demand coordinated interactions between a wide assortment of lipid and protein molecules that dynamically link to the cortical actin cytoskeletons and the plasma membrane.[8]

In the past two decades, "nanomedicine" has attracted much attention among researchers in the fields of drug delivery, gene therapy, and diagnosis.[9−12] Considering that these delivery systems are intended to deliver drugs and genes to the cytosol, nucleus, or other specific intracellular compartments, navigating the endocytosis process is critical to their success. Consequently, designing efficient and safe delivery systems for biomedical applications requires a comprehensive understanding of their endocytosis processes.

Recognition of nanoparticles on a cell surface and the following endocytosis depend on the type, size, and surface properties of the nanoparticles. From the viewpoint of the size of nanoparticles, Ding et al. found that the size of the gold nanospheres was an important factor for their uptake into cells. The uptake of gold nanospheres of 15 nm in diameter was higher than those of 45 and 80 nm.[13] Malugin et al. observed that larger amounts of amorphous silica nanoparticles of 100 nm were internalized by epithelial cells than those of 50, 200, and 500 nm.[14] In addition, surface properties also affect the cellular uptake. Surface charge[15−18] and the type of modified molecules[19−22] have an impact on the cellular uptake. The

Received: October 22, 2020
Accepted: December 1, 2020
Published: December 10, 2020

https://dx.doi.org/10.1021/acsomega.0c05162
ACS Omega 2020, 5, 32744−32752

shape of the nanoparticles is also an important factor for cellular uptake. As a result of examining endocytosis pathways of gold nanoparticles in the forms of stars, rods, and triangles into RAW 264.7 cells, the pathways were found to be different and depended on their shapes.[18,23] Herd et al. also observed that the shape of silica nanoparticles (the worm-like, cylindrical, and spherical) influenced their endocytosis pathways in A549 cells and RAW 264.7 cells.[24] For rod-like nanoparticles, Liu et al. examined nanorods with different aspect ratios based on the tobacco mosaic virus for their uptake by HeLa cells and human umbilical vein endothelial cells (HUVECs).[25] They found that the aspect ratio had a considerable effect on the cellular uptake by the respective cells. The shapes and surface charge of silica nanotubes have also been assessed for their cellular uptake.[26] Gold nanorods with different aspect ratios were also examined to clarify differences in uptake by HeLa cells.[27]

Thus, the relationship between surface properties of nanoparticles and cellular uptake has been examined mostly using established cell lines. However, the established cell lines generally originate from cancer cells or are transformed from normal cells into immortalized cells.[28] Therefore, primary cells may give us more reliable information about the endocytosis process of nanoparticles into cells, and their use should allow the quantitative analysis of the internalization of nanoparticles into particular cells and observation by time-course microscopy studies.

The objectives of this study are to understand the relationship between surface properties of nanoparticles and the induced endocytosis pathway in several types of cells, including primary cells and established cell lines. All the gold nanorods (AuNRs) used in this study had a similar aspect ratio. Furthermore, we utilized surface modifications of AuNRs that have already been established, for example, modification with polyethylene glycol,[29,30] poly(styrene sulfonic acid) (PSS),[31,32] poly(allylamine hydrochloride) (PAH),[31] silica,[33−35] and aminated silica.[35,36] More importantly, gold can be precisely quantified by inductively coupled plasma optical emission spectrometry (ICP−OES) with higher sensitivity in trace-level concentrations and higher accuracy, compared with fluorescence analysis carried out in the case of polymer nanoparticles modified with a fluorescent dye.[37−39]

In this study, we employed AuNRs modified with polymers and silica layers as model nanoparticles to obtain nanoparticles with positive and negative charges. Using these AuNRs, the cellular uptake by several types of cells was quantified by ICP−OES. Using endocytosis inhibitors, we further investigated the endocytosis mechanisms and their differences caused by the surface properties and cell types.

RESULTS AND DISCUSSION

Modification and Characterization of AuNRs. To evaluate the impact of different surface modifications on the cellular uptake of AuNRs, four kinds of AuNRs with different chemical properties and surface charges, namely, PSS AuNRs (polymer modification, anionic), PAH AuNRs (polymer modification, cationic), silica AuNRs (silica modification, anionic), and amine−silica AuNRs (silica modification, cationic) were prepared. Transmission electron microscopy (TEM) images (Figure 1A−D) revealed that AuNRs were uniform in shape, and the mean size was about 70 nm in length and 10 nm in width. Size distribution of the AuNRs measured from the TEM images is shown in Figure 1E. The polymer

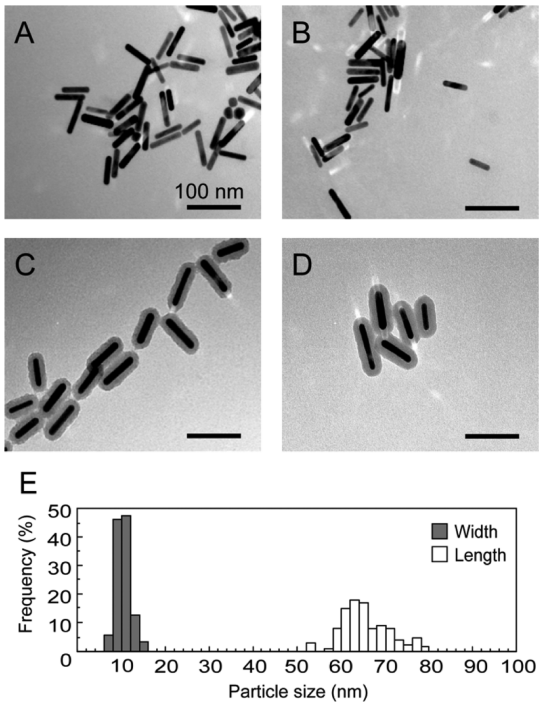

Figure 1. TEM images of PSS (A), PAH (B), silica (C), and amine−silica (D) AuNRs. Scale bars indicate 100 nm. Size distribution of AuNRs measured from the TEM images (E).

layers of PSS AuNRs and PAH AuNRs could not be observed because they were invisibly thin in TEM observation (Figure 1A,B),[40] meaning that the amount of the coated polymers was low enough to be ignorable compared with the gold nanorods. The silica shell can be estimated to have a uniform thickness of 10 nm. The absorption spectra with vis−NIR spectrometry are shown in Figure 2. The AuNRs had two absorption bands,

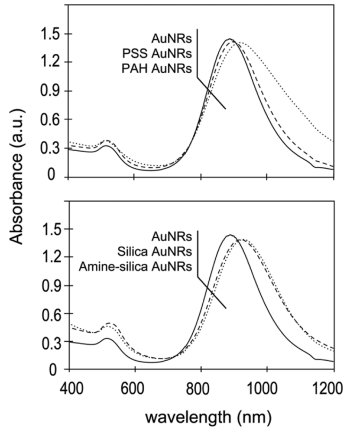

Figure 2. Vis−NIR spectrum of AuNRs with different modifications.

around 550 nm (transverse plasmon resonance) and 900 nm (longitudinal plasmon resonance). After the surface modifications, a slight red shift of the absorption in the near-infrared light region was observed, which agrees with previous reports.[41,42] The surface modifications were also confirmed by measuring the zeta potentials (Table 1). PSS AuNRs and silica AuNRs showed negative zeta potentials, and PAH AuNRs and amine−silica AuNRs showed positive zeta potentials.

https://dx.doi.org/10.1021/acsomega.0c05162
ACS Omega 2020, 5, 32744−32752

Table 1. Coating Sequence and Resulting Zeta Potential

name	surface structure	zeta potential (mV)
PSS AuNRs	sulfonate	−43.33 ± 0.65
PAH AuNRs	amine	+37.31 ± 1.16
silica AuNRs	silanol	−27.62 ± 0.58
amine−silica AuNRs	amine	+29.19 ± 0.92

Cytotoxicities of AuNRs with different modifications. Before evaluating the uptake of these surface-modified AuNRs by cells, their cytotoxicities were examined to exclude secondary effects of the toxicity on the uptake. In this study, two kinds of primary cells, HUVECs and human primary monocyte-derived macrophages, and two kinds of established cell lines, murine macrophages (RAW 264.7: RAW cells) and human cervical cancer cells (HeLa cells), were used. For the primary cells, human monocyte-derived macrophages (HMDMs) are used as model cells to understand various functions of macrophages. We previously established a method of differentiation from human peripheral monocytes to the macrophages by stimulating with GM−CSF or M−CSF.[43] HUVECs are the most commonly used endothelial cells and chosen as a counterpart of HMDMs. For the established cell lines, RAW cells originated from murine macrophages are chosen as a counterpart of HMDMs in terms of the macrophage origin. HeLa cells are generally established cell lines and often used for research of endocytosis.

We varied the concentrations of the coated AuNRs in a wide range, including some that were higher than those published in a systematic study of the endocytosis of AuNRs.[14] The experiments were conducted in serum-free media in order to minimize nonspecific interaction of serum proteins that may affect the surface properties of the AuNRs and alter the interactions between the AuNRs and cellular surface.[16,17]

The cationic AuNRs (PAH and amine−silica AuNRs) showed higher cytotoxicity than the anionic AuNRs (PSS and silica AuNRs) in all types of cells (Figure 3). It would be because of the electrostatic interaction between the cationic nanoparticles and the anionic cell surfaces.[16] The polymer-modified AuNRs (PSS and PAH AuNRs) tended to show slightly higher toxicity than the silica-modified AuNRs (silica and amine−silica AuNRs) regardless of the cell type. From the point of view of the cell type, HUVECs and RAW cells were more sensitive to AuNRs compared with HeLa cells and HMDMs. The cell viability of HeLa cells at a high concentration of AuNRs (12 μg/mL) was still around 80%, while significant toxicities were observed in the other types of cells at that concentration. For HUVECs, the concentration of AuNRs needed to be below 6 μg/mL for cell viability to reach 80%. Overall, 6.0 μg/mL AuNRs was the highest concentration that did not show significant toxicity and can be considered an inert concentration for cellular endocytosis. Therefore, 6.0 μg/mL was chosen as the working concentration for cellular uptake experiments.

Cellular Uptake of AuNRs with Different Modifications. The time course of cellular uptake of AuNRs with different modifications was examined at 1, 4, 8, 12, and 24 h (Figure 4). At the beginning stage (1 h), the amount of uptake was similar (about 0.2 μg/10^5 cells, corresponding to 1.8×10^4 gold nanorods in one cell) for all kinds of cells. At the middle stage of incubation (4 to 12 h), the uptake of cationic AuNRs (PAH and amine−silica AuNRs) was higher than that of anionic AuNRs (PSS and silica AuNRs), especially for HUVECs, HMDMs, and HeLa cells, presumably because of the difference in the mode of electrostatic interaction with anionic proteoglycans on the cell surface.[44] Thus, the surface charges of AuNRs, but not the thickness and chemical structure of the modification, are a dominant factor to affect their uptake. After that, the uptake behaviors of AuNRs with different modifications in different cell types were complicated.

HUVECs are the most commonly used endothelial cells in the published research.[45] HMDMs are also used as model cells of macrophages, which play a key role in inflammation and protecting the organism from infection.[46] From our results, HMDMs actively ingested AuNRs in a 1.4-fold greater amount compared with HUVECs at 24 h. The difference would be reflected by that of their original characteristics in the human body. When we compared HMDMs with RAW cells, established from murine macrophages, the amount of gold in the RAW cells was about half that of HMDMs. HeLa cells also showed uptake of AuNRs comparable with that of HMDMs.

To verify that the detected gold originated from AuNRs internalized into cells by endocytosis and not cell surface-adsorbed AuNRs, examinations of the effects of incubation at 4 °C and with sodium azide were performed (Figure 5). Endocytosis is an ATP-driven, energy-dependent cellular event, and the abovementioned treatments should deplete cellular ATPs and inhibit the endocytic uptake of AuNPs.[47] In both treatments, the cellular uptakes of all kinds of AuNRs were inhibited to 20% in all kinds of cells, indicating that AuNRs were internalized into cells by endocytosis and the amount of AuNRs existing on the cell surface was ignorable.

Endocytosis Pathway of AuNRs. Energy-dependent uptake pathways for nanoparticle internalization are mainly categorized into macropinocytosis, clathrin-mediated endocytosis, and caveolae-mediated endocytosis.[48] To know by which endocytosis pathways AuNRs with different modifications were internalized into cells, the effects of inhibitors corresponding to these endocytosis pathways on their uptakes were examined (Figure 6). Amiloride, an inhibitor of macropinocytosis, lowers

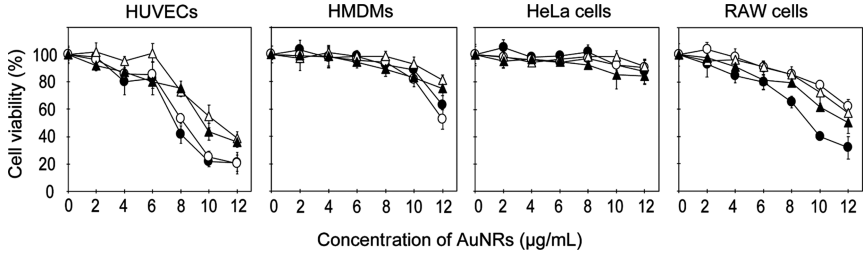

Figure 3. Cytotoxicities of the AuNRs. Cells were exposed to AuNRs modified with PSS(○), PAH (●), silica (△), and amine−silica (▲) for 24 h. Data represent mean values for n = 3, and error bars are one standard deviation of the means.

https://dx.doi.org/10.1021/acsomega.0c05162
ACS Omega 2020, 5, 32744−32752

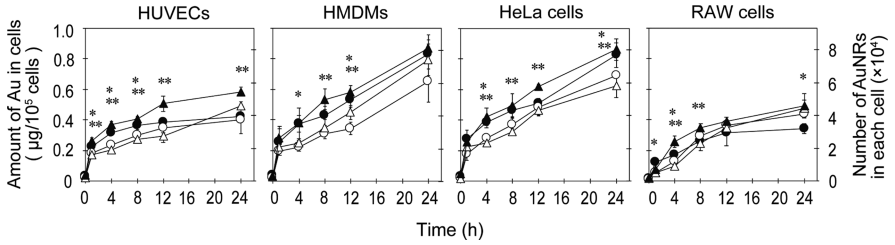

Figure 4. Cellular uptake of AuNRs modified with PSS(○), PAH (●), silica (△), and amine−silica (▲). The cells were incubated with 6 μg/mL AuNRs with different modifications for 1, 4, 8, 12, and 24 h. Data represent mean values for $n = 3$, and the error bars are one standard deviation of the means. Statistical significance: *$P < 0.05$ compared with values of PSS AuNRs for PAH AuNRs, **$P < 0.05$ compared with values of silica AuNRs for amine−silica AuNRs (student's t-test).

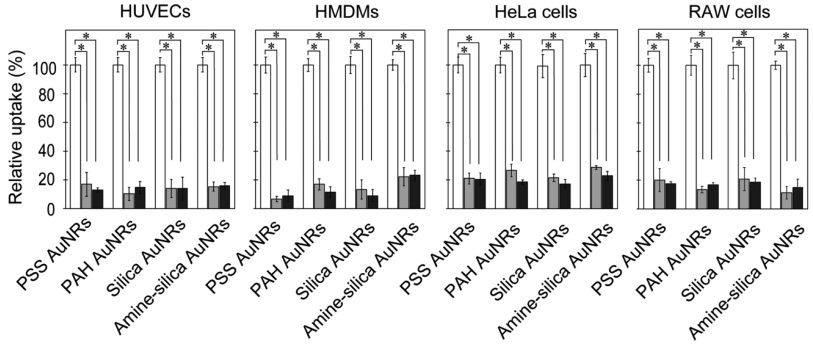

Figure 5. Effect of 4 °C incubation and sodium azide on the uptake of AuNRs with different modifications by cells. These cells were treated at 4 °C (gray bars) in the presence of sodium azide (closed bars) for 45 min. The cellular uptake of AuNRs was normalized to cells without inhibition treatment (open bars). Data represent mean values for $n = 3$, and error bars are one standard deviation of the means. Statistical significance: *$P <$ 0.01 compared with values for treated cells at 4 °C and with sodium azide (student's t-test).

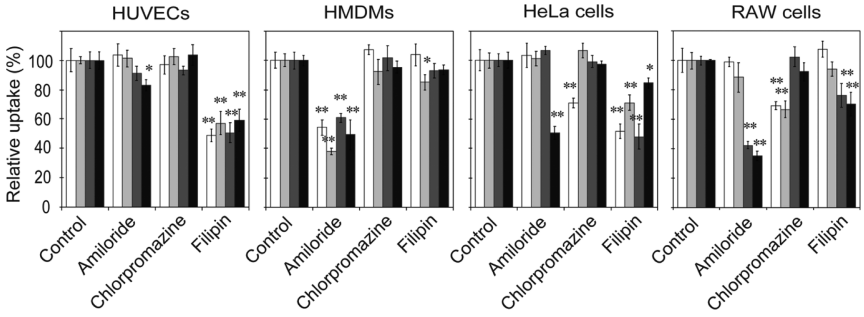

Figure 6. Effect of endocytosis inhibitors on the uptake of AuNRs with different modifications by cells. The cells were exposed to endocytosis inhibitors for 45 min, and then, the medium was replaced with fresh medium containing AuNRs for 1 h. The uptake of AuNRs was normalized to that of cells without inhibition treatment. Open, light gray, dark gray, and closed bars indicate uptake of PSS, PAH, silica, and amine−silica AuNRs, respectively. Data represent mean values for $n = 3$, and error bars are one standard deviation of the means. Statistical significance: *$P < 0.05$ and **$P < 0.01$ when compared with values for control and other inhibitors (Dunnett's test).

submembranous pH and impairs actin polymerization by preventing Rac1 and Cdc42 signaling, which is important for macropinocytosis.[49,50] Chlorpromazine, an inhibitor of clathrin-mediated endocytosis, inhibits the formation of a clathrin-coated pit via an invertible translocation of clathrin and its adapter proteins from the plasma membrane to intracellular vesicles.[51] Filipin, an inhibitor of caveolae-mediated endocytosis, binds to cholesterol in caveolae and forms ultrastructural aggregates and complexes.[52]

As shown in Figure 6, for HUVECs, the cellular uptake of all kinds of AuNRs was inhibited by filipin only, suggesting that these AuNRs were internalized mainly by caveolae-mediated endocytosis regardless of their surface modification. This is reasonably well supported by reports that caveolae are abundant in endothelial cells,[53] and caveolin-1 and caveolae are involved in the regulation of the endothelial cell function.[54] For HMDMs, the cellular uptake was inhibited by amiloride only. The results suggested that AuNRs were most likely internalized by macropinocytosis regardless of their surface modifications. This specific form of macropinocytosis allows macrophages to consistently capture antigenic substances and pathogens as part of their immuno-defense functions. Surprisingly, regardless of the surface alteration, these AuNPs may share similar uptake pathways into these primary cells.

In contrast, the modes of inhibition in AuNR uptake in the established cell lines (HeLa and RAW cells) were more complicated and dependent on surface modifications. For HeLa cells, the uptakes of PSS AuNRs and amine−silica AuNRs were inhibited by chlorpromazine and amiloride, respectively. The result suggested that clathrin-mediated

https://dx.doi.org/10.1021/acsomega.0c05162
ACS Omega 2020, 5, 32744−32752

endocytosis and macropinocytosis contributed to the uptake of PSS AuNRs and amine−silica AuNRs, respectively. Filipin inhibited uptake of all kinds of AuNRs, suggesting that caveolae-mediated endocytosis contributed to the uptake of AuNRs regardless of surface modifications. For RAW cells, the uptakes of silica and amine−silica AuNRs were inhibited by both amiloride and filipin, suggesting that silica AuNRs and amine−silica AuNRs were internalized by RAW cells via both macropinocytosis and caveolae-mediated endocytosis. The uptakes of PSS and PAH AuNRs were inhibited by chlorpromazine, an inhibitor of clathrin-mediated endocytosis. In the case of RAW cells, multiple endocytosis pathways may contribute to the uptake of AuNRs, depending on their surface modifications.

Macropinocytosis is an induced form of endocytosis that facilitates cellular uptake of extracellular materials and solutes, and thus, induction of micropinocytosis may increase the uptake of AuNRs into cells. To evaluate the possibility, we pretreated the cells with recombinant human stromal cell-derived factor (SDF)-1α (CXCL12), which is known to activate macropinocytosis (Figure 7).[55] SDF-1α led to a

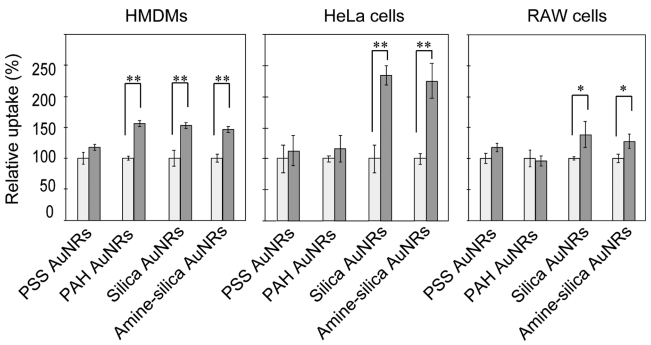

Figure 7. Effect of SDF-1α on uptake of AuNRs with different modifications by cells. The cells were exposed to SDF-1α for 30 min; then, the medium was replaced with a fresh medium containing AuNRs for 1 h. The uptake of AuNRs was normalized to that of cells without SDF-1α treatment. Open and closed bars indicate uptake under the control condition without SDF-1α and in the presence of SDF-1α, respectively. Data represent mean values for $n = 3$, and error bars are standard deviation for means. Statistical significance: $^*P < 0.05$ and $^{**}P < 0.01$ compared with values for control cells without SDF-1α treatment (student's t-test).

significant enhancement in cellular uptake of AuNRs by HMDMs with the exception of PSS AuNRs, yielding a 1.5-fold greater AuNR uptake relative to cells without SDF-1α treatment. In HeLa cells, a twofold increase was observed in silica and amine−silica AuNR uptake after the treatment with SDF-1α. A similar tendency was observed for the AuNR uptake by RAW cells. These results suggest the potential effect of macropinocytosis induction in promoting nanoparticle delivery into cells.

CONCLUSIONS

We examined the endocytic uptake pathways by which AuNRs enter cells and how their surface properties and cell-type difference impact them. AuNRs were modified with a polymer or silica to become anionic or cationic. In this study, we employed the AuNRs with different surface modifications as a model set of nanoparticles with different surface modifications. The human primary cells (HUVECs and HMDMs) showed a unimodal uptake of AuNRs regardless of their surface modification. This may be attributed to the intrinsic characters of the original cells. In contrast, in the case of established cell lines (HeLa and RAW cells), AuNRs were internalized by multiple endocytosis pathways, and it depended on surface properties (Figure 8). HeLa cells are frequently used as a

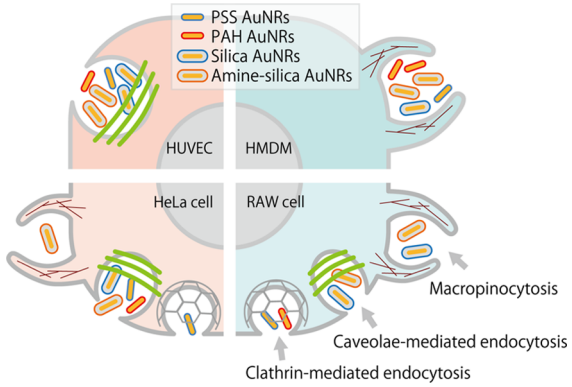

Figure 8. Schematic illustration of the endocytosis mechanisms of AuNRs with different surface modifications.

model cell to study endocytosis. However, as shown in this study, there can be considerable cell-type dependencies in the modes of cellular uptake, suggesting the importance of cell-type selection in studying the modes of cellular uptake of nanoparticles. Primary cells may illustrate cellular uptake behaviors closer to in vivo and should be used where available. Further examination using other types of nanoparticles, for example, different sizes and shapes of gold nanoparticles, polymer nanoparticles, liposomes, and other nanomaterials, will give us a deeper understanding of the modes of endocytosis related to the immune system, communication between cells via extracellular vesicles, and other cellular processes. Looking at the in vivo drug delivery system mediated by nanomaterials, their uptake by target cells would be affected by lots of factors, that is, circulating stability of the nanomaterials, distribution in the microenvironment of targeted organs, and recognition by target cells.[29,56,57] Although it is complicated, basic knowledge for endocytosis in the cellular level will be essential to develop efficient delivery systems of therapeutic molecules that work in cells.

EXPERIMENTAL PROCEDURES

Materials. AuNRs were provided by Dai Nippon Toryo Co. Ltd. (Osaka, Japan). PSS sodium salt and PAH were purchased from Alfa Aesar (Lancashire, UK). Thiol-terminated poly (ethylene glycol) (PEG, MW 5000 Da) was purchased from NOF Co., Ltd. (Tokyo, Japan). Tetraethyl orthosilicate (TEOS) was purchased from Kasei Kogyo (Tokyo, Japan). (3-Aminopropyl) triethoxysilane (APTES) was purchased from Kanto Kagaku (Tokyo, Japan). Ethanol (99%), ammonia solution (28%), hydrochloric acid, and nitric acid were purchased from FUJIFILM Wako Pure Chemical Industries (Osaka, Japan). Amiloride hydrochloride and Filipin III were purchased from Cayman Chemical (Michigan, USA). Chlorpromazine hydrochloride was purchased from Tokyo Chemical Industry Co., Ltd. (Tokyo, Japan). Recombinant human CXCL12 (SDF-1α) was purchased from Biolegend (San Diego, USA). Cell counting kit-8 (CCK-8) was purchased from Dojindo Laboratories (Kumamoto, Japan).

https://dx.doi.org/10.1021/acsomega.0c05162
ACS Omega 2020, 5, 32744−32752

Surface Modification of AuNRs. AuNRs stabilized by cetyltrimethylammonium bromide (CTAB) were modified with layers of polyelectrolytes as per a previous report.[58,59] The first layer was PSS, which is negatively charged, and the second layer is PAH, which is positively charged. Overall, two kinds of polymer-coated AuNRs were obtained by layer-by-layer methods. Briefly, a solution of AuNRs containing excess CTAB was centrifuged at 12 ,000 ×*g* for 15 min, decanted, and resuspended in MQ water to remove the excess CTAB. Then, 8 mL of a solution of 1 mM AuNRs (concentration on the basis of gold atoms) and 200 μL of PSS solution (50 mg/mL in MQ water) were added into 1.8 mL of MQ water, and the mixed solution was then vortexed vigorously for 3 min. After standing for 12 h, the excess PSS molecules in the supernatant fraction were removed by centrifugation twice, and the pellet was redispersed in 10 mL of MQ water. For PAH modification, 200 μL of the PAH solution (10 mg/mL in MQ water) was added into 1 mL of the PSS AuNR solution, and the mixed solution was then vortexed vigorously for 3 min. After standing for 12 h, the excess PAH molecules in the supernatant fraction were removed by centrifugation twice, and the pellet was redispersed in 1 mL of MQ water. The obtained PAH/PSS AuNRs (abbreviated as PAH AuNRs) could then be used for cell experiments.

Silica-modified AuNRs were prepared by a method previously reported.[41] A solution of AuNRs containing excess CTAB was centrifuged at 12 ,000 ×*g* for 15 min, decanted, and resuspended in MQ water to remove the excess CTAB. A total of 10 mL of a solution of 1 mM AuNRs (concentration on the basis of gold atoms) was added to 2 mL of 1 mM thiol-terminated PEG (MW. 5000 Da). The mixture was stirred overnight at room temperature and was dialyzed. PEG-modified AuNRs were coated with a silica layer using the modified Stöber method, which is based on the hydrolysis of TEOS in the ethanol/water mixture in the presence of AuNRs. A total of 1 mL of a solution of 10 mM PEG-modified AuNRs (on the basis of gold atoms) was diluted with 7.8 mL of ethanol. The mixture was added to 40 μL of 28% ammonia solution, and 1 mL of 50 mM TEOS was added. The reaction was allowed to proceed for 24 h at room temperature. The silica layer on the AuNRs (abbreviated as silica AuNRs) was further modified with APTES.[36] Briefly, 1 mL of a solution of 10 mM silica AuNRs was concentrated by centrifugation and then dispersed in 4 mL of ethanol. Next, 28 μL of APTES and 20 μL of 28% ammonia solution were then added. The mixture was allowed to react for 24 h at room temperature, and the product was collected by centrifugation and washed with ethanol twice. The pellet of amine−silica AuNRs was dispersed in 1 mL of MQ water and could then be used for cell experiments.

Characterization of AuNRs. The shape and size of AuNRs were observed by transmission electron microscopy (TEM, (JEOL-2100F; JEOL, Japan). The absorption spectra were characterized with a UV−vis−NIR spectrophotometer (V-670; Jasco, Tokyo, Japan). The zeta potentials of the AuNRs were measured using a Zetasizer (Malvern Zetasizer Nano ZS; Malvern Instruments Ltd, Malvern, UK).

Cell Culture. Human peripheral blood mononuclear cells (PBMC) were obtained from healthy volunteers, and written informed consent was obtained from all the donors. All protocols using human materials were approved by the Kumamoto University review board (no.486) and were conducted in accordance with the approved guidelines. Monocytes were isolated using Lymphoprep and then stimulated with GM−CSF (5 ng/mL) or M−CSF (100 ng/mL) for seven days to differentiate them into HMDMs.[43] HMDMs were cultured in DMEM (low glucose) supplemented with 2% FBS and 100 mg/mL penicillin and streptomycin. HUVECs were cultured in endothelial cell growth medium under a humidified 5% CO_2 at 37 °C. RAW 264.7 cells and HeLa cells were cultured in DMEM (high glucose) with 10% FBS under a humidified 5% CO_2 at 37 °C.

Cell Viability Assays. Cell viability assays were measured using a cell counting kit-8 (CCK-8, Dojindo Laboratories, Japan) following the manufacturer's instructions. Typically, around 8000 cells per well were seeded onto 96-well plates with a culture medium containing 10% FBS and cultured overnight. After incubation, the cells were then exposed to AuNRs with different surface modifications (6.0 μg/mL on the basis of gold atoms) for 24 h in the culture medium without serum. Then, the cell viability of each well was determined by treatment with the CCK-8 kit following the manual. The absorbance was determined using a microplate reader (680; Bio-Rad, Hercules, CA) at 450 nm.

Evaluation of the Amount of Internalized AuNRs in Cells. Four types of cells (10^5 cells/well) were seeded onto a six-well plate and cultured with a medium containing 10% FBS. After incubation overnight, cells were incubated with AuNRs with different surface modifications (6.0 μg/mL on the basis of gold atoms) in the medium without serum for 1, 4, 8, 12, and 24 h. After the allotted time, the cells were rinsed thoroughly with cold PBS and collected. For the quantitative determination of the Au content in the cells, atomic absorption spectroscopy analysis was used after the collected cells were digested by aqua regia.[60] Briefly, a 100 μL solution of the collected cells were digested with 900 μL of aqua regia (3:1 ratio HCl/HNO_3) overnight. Then, the mixture was dried by a dry block bath (Dry Block Bath THB-2, AS ONE Corporation, Osaka, Japan) at 98 °C. The pellet was dispersed in a 2 mL solution of 1% HCl, and the Au content was analyzed by ICP−OES (Thermo iCAP 7000 series ICP spectrometer; Thermo Fisher Scientific, MA). The mean size of the gold nanorods used in this study was about 70 nm in length and 10 nm in width. From the density of gold (19.32 g/cm^3) or the size of the crystal lattice (0.4078 nm for four gold atoms),[61] the number of gold atoms in one gold nanorod can be calculated to be 3.47×10^5. The amount of internalized gold nanorods was shown as "μg of gold per 10^5 cells" and "number of gold nanorods in one cell".

Evaluation of the Endocytosis Mechanism. To understand the uptake mechanism of AuNRs, cells were seeded onto six-well plates (10^5 cells/well) in the medium with 10% FBS. After overnight incubation, the cells were treated with one of the following treatments prior to the AuNR exposure: (1) at 4 °C for 45 min, (2) in the presence of 10 mM sodium azide for 45 min, (3) in the presence of 100 μg/mL amiloride (inhibits macropinocytosis) for 45 min, (4) in the presence of 7.5 μg/mL chlorpromazine (inhibits clathrin-mediated endocytosis) for 45 min, (5) in the presence of 5 μg/mL filipin (inhibits caveolae-mediated endocytosis) for 45 min, and (6) in the presence of 100 nM SDF-1α (activates macropinocytosis) for 30 min. After treatment, the medium was replaced with a fresh medium, which was without serum and contained the AuNRs with different surface modifications (6 μg/mL on the basis of gold atoms) for 1 h. After that, the cells were washed with cold PBS three times, trypsinized, and collected for measurement by

https://dx.doi.org/10.1021/acsomega.0c05162
ACS Omega 2020, 5, 32744−32752

ICP−OES. The cellular uptake of AuNRs was normalized to cells without inhibition treatment.

AUTHOR INFORMATION

Corresponding Author

Takuro Niidome − *Faculty of Advanced Science and Technology, Kumamoto University, Kumamoto 860-8555, Japan*; orcid.org/0000-0002-8070-8708; Email: niidome@kumamoto-u.ac.jp

Authors

Yuxiang Xiao − *Faculty of Advanced Science and Technology, Kumamoto University, Kumamoto 860-8555, Japan*

Wei Xu − *Faculty of Advanced Science and Technology, Kumamoto University, Kumamoto 860-8555, Japan*

Yoshihiro Komohara − *Department of Cell Pathology, Graduate School of Medical Sciences, Kumamoto University, Kumamoto 860-8556, Japan*

Yukio Fujiwara − *Department of Cell Pathology, Graduate School of Medical Sciences, Kumamoto University, Kumamoto 860-8556, Japan*

Hisaaki Hirose − *Institute for Chemical Research, Kyoto University, Uji, Kyoto 611-0011, Japan*; orcid.org/0000-0001-6301-2760

Shiroh Futaki − *Institute for Chemical Research, Kyoto University, Uji, Kyoto 611-0011, Japan*; orcid.org/0000-0002-0124-4002

Complete contact information is available at: https://pubs.acs.org/10.1021/acsomega.0c05162

Author Contributions

X. Y. performed the experiments and analyzed the data. W. X., H. H., and S. F. advised on the cellular experiments. Y. K. and Y. F. supported the isolation and cell culture of HMDMs. W. X. supported with manuscript writing. T. N. designed the experiments, analyzed the data, and wrote the paper with X. Y., W. X., H. H., and S. F..

Notes

The authors declare no competing financial interest.

ACKNOWLEDGMENTS

This research was funded by Japan Science and Technology Agency (JST), Core Research for Evolutional Science and Technology (CREST) (grant number JPMJCR18H5). We thank James Murray PhD of the Edanz Group (https://en-author-services.edanzgroup.com/ac) for editing a draft of this manuscript.

ABBREVIATIONS

AuNRs, gold nanorods; PSS, poly(styrenesulfonate); PAH, poly(allylamine hydrochloride); PBMC, human peripheral blood mononuclear cells; HMDMs, human monocyte-derived macrophages; HUVECs, human umbilical vein endothelial cells; SDF-1α, stromal cell-derived factor 1 alpha, also known as recombinant CXCL12

REFERENCES

(1) Manzanares, D.; Ceña, V. Endocytosis: The nanoparticle and submicron nanocompounds gateway into the cell. *Pharmaceutics* **2020**, *12*, 371.

(2) Behzadi, S.; Serpooshan, V.; Tao, W.; Hamaly, M. A.; Alkawareek, M. Y.; Dreaden, E. C.; Brown, D.; Alkilany, A. M.; Farokhzad, O. C.; Mahmoudi, M. Cellular uptake of nanoparticles: journey inside the cell. *Chem. Soc. Rev.* **2017**, *46*, 4218−4244.

(3) Sigismund, S.; Confalonieri, S.; Ciliberto, A.; Polo, S.; Scita, G.; Di Fiore, P. P. Endocytosis and signaling: cell logistics shape the eukaryotic cell plan. *Physiol. Rev.* **2012**, *92*, 273−366.

(4) Sarantis, H.; Grinstein, S. Subversion of phagocytosis for pathogen survival. *Cell Host Microbe* **2012**, *12*, 419−431.

(5) Ding, X.; Xiang, S. Endocytosis and human innate immunity. *J. Immunol. Res.* **2018**, *2*, 65−70.

(6) Bloomfield, G.; Kay, R. R. Uses and abuses of macropinocytosis. *J. Cell Sci.* **2016**, *129*, 2697−2705.

(7) Conner, S. D.; Schmid, S. L. Regulated portals of entry into the cell. *Nature* **2003**, *422*, 37−44.

(8) Kumari, S.; Mg, S.; Mayor, S. Endocytosis unplugged: multiple ways to enter the cell. *Cell Res.* **2010**, *20*, 256−275.

(9) McNamara, K.; Tofail, S. A. M. Nanoparticles in biomedical applications. *Adv. Phys.: X* **2017**, *2*, 54−88.

(10) Yan, C.; Quan, X.-J.; Feng, Y.-M. Nanomedicine for gene delivery for the treatment of cardiovascular diseases. *Curr. Gene Ther.* **2019**, *19*, 20−30.

(11) Alex, S. M.; Sharma, C. P. Nanomedicine for gene therapy. *Drug Delivery Transl. Res.* **2013**, *3*, 437−445.

(12) Issa, B.; Obaidat, I.; Albiss, B.; Haik, Y. Magnetic nanoparticles: surface effects and properties related to biomedicine applications. *Int. J. Mol. Sci.* **2013**, *14*, 21266−21305.

(13) Ding, L.; Yao, C.; Yin, X.; Li, C.; Huang, Y.; Wu, M.; Wang, B.; Guo, X.; Wang, Y.; Wu, M. Size, shape, and protein corona determine cellular uptake and removal mechanisms of gold nanoparticles. *Small* **2018**, *14*, 1801451.

(14) Malugin, A.; Herd, H.; Ghandehari, H. Differential toxicity of amorphous silica nanoparticles toward phagocytic and epithelial cells. *J. Nanopart. Res.* **2011**, *13*, 5381.

(15) Fröhlich, E. The role of surface charge in cellular uptake and cytotoxicity of medical nanoparticles. *Int. J. Nanomed.* **2012**, *7*, 5577−5591.

(16) Hauck, T. S.; Ghazani, A. A.; Chan, W. C. W. Assessing the effect of surface chemistry on gold nanorod uptake, toxicity, and gene expression in mammalian cells. *Small* **2008**, *4*, 153−159.

(17) Sun, Q.; Shi, X.; Feng, J.; Zhang, Q.; Ao, Z.; Ji, Y.; Wu, X.; Liu, D.; Han, D. Cytotoxicity and cellular responses of gold nanorods to smooth muscle cells dependent on surface chemistry coupled action. *Small* **2018**, *14*, 1803715.

(18) Arnida; Janát-Amsbury, M. M.; Ray, A.; Peterson, C. M.; Ghandehari, H. Geometry and surface characteristics of gold nanoparticles influence their biodistribution and uptake by macrophages. *Eur. J. Pharm. Biopharm.* **2011**, *77*, 417−423.

(19) Rayavarapu, R. G.; Petersen, W.; Hartsuiker, L.; Chin, P.; Janssen, H.; van Leeuwen, F. W. B.; Otto, C.; Manohar, S.; van Leeuwen, T. G. In vitro toxicity studies of polymer-coated gold nanorods. *Nanotechnology* **2010**, *21*, 145101.

(20) Hao, Y.; Yang, X.; Song, S.; Huang, M.; He, C.; Cui, M.; Chen, J. Exploring the cell uptake mechanism of phospholipid and polyethylene glycol coated gold nanoparticles. *Nanotechnology* **2012**, *23*, 045103.

(21) Jiang, Y.; Huo, S.; Mizuhara, T.; Das, R.; Lee, Y.-W.; Hou, S.; Moyano, D. F.; Duncan, B.; Liang, X.-J.; Rotello, V. M. The interplay of size and surface functionality on the cellular uptake of sub-10 nm gold nanoparticles. *ACS Nano* **2015**, *9*, 9986−9993.

(22) Alkilany, A. M.; Nagaria, P. K.; Hexel, C. R.; Shaw, T. J.; Murphy, C. J.; Wyatt, M. D. Cellular uptake and cytotoxicity of gold nanorods: molecular origin of cytotoxicity and surface effects. *Small* **2009**, *5*, 701−708.

(23) Xie, X.; Liao, J.; Shao, X.; Li, Q.; Lin, Y. The effect of shape on cellular uptake of gold nanoparticles in the forms of stars, rods, and triangles. *Sci. Rep.* **2017**, *7*, 3827.

(24) Herd, H.; Daum, N.; Jones, A. T.; Huwer, H.; Ghandehari, H.; Lehr, C.-M. Nanoparticle geometry and surface orientation influence mode of cellular uptake. *ACS Nano* **2013**, *7*, 1961−1973.

(25) Liu, X.; Wu, F.; Tian, Y.; Wu, M.; Zhou, Q.; Jiang, S.; Niu, Z. Size dependent cellular uptake of rod-like bionanoparticles with different aspect ratios. *Sci. Rep.* **2016**, *6*, 24567.
(26) Nan, A.; Bai, X.; Son, S. J.; Lee, S. B.; Ghandehari, H. Cellular uptake and cytotoxicity of silica nanotubes. *Nano Lett.* **2008**, *8*, 2150−2154.
(27) Fernando, D.; Sulthana, S.; Vasquez, Y. Cellular uptake and cytotoxicity of varying aspect ratios of gold nanorods in HeLa cells. *ACS Appl. Bio Mater.* **2020**, *3*, 1374−1384.
(28) Königs, M.; Lenczyk, M.; Schwerdt, G.; Holzinger, H.; Gekle, M.; Humpf, H.-U. Cytotoxicity, metabolism and cellular uptake of the mycotoxin deoxynivalenol in human proximal tubule cells and lung fibroblasts in primary culture. *Toxicology* **2007**, *240*, 48−59.
(29) Niidome, T.; Yamagata, M.; Okamoto, Y.; Akiyama, Y.; Takahashi, H.; Kawano, T.; Katayama, Y.; Niidome, Y. PEG-modified gold nanorods with a stealth character for in vivo applications. *J. Controlled Release* **2006**, *114*, 343−347.
(30) Niidome, T.; Ohga, A.; Akiyama, Y.; Watanabe, K.; Niidome, Y.; Mori, T.; Katayama, Y. Controlled release of PEG chain from gold nanorods: targeted delivery to tumor. *Bioorg. Med. Chem.* **2010**, *18*, 4453−4458.
(31) Hauck, T. S.; Ghazani, A. A.; Chan, W. C. W. Assessing the effect of surface chemistry on gold nanorod uptake, toxicity, and gene expression in mammalian cells. *Small* **2008**, *4*, 153−159.
(32) Yin, F.; Yang, C.; Wang, Q.; Zeng, S.; Hu, R.; Lin, G.; Tian, J.; Hu, S.; Lan, R. F.; Yoon, H. S.; Lu, F.; Wang, K.; Yong, K.-T. A light-driven therapy of pancreatic adenocarcinoma using gold nanorods-based nanocarriers for co-delivery of doxorubicin and siRNA. *Theranostics* **2015**, *5*, 818−833.
(33) Akiyama, Y.; Niidome, Y.; Mori, T.; Katayama, Y.; Niidome, T. PEG-silica-modified gold nanorods that retain their optical properties in tumor tissues. *J. Biomater. Sci., Polym. Ed.* **2013**, *24*, 2071−2080.
(34) Shen, S.; Tang, H.; Zhang, X.; Ren, J.; Pang, Z.; Wang, D.; Gao, H.; Qian, Y.; Jiang, X.; Yang, W. Targeting mesoporous silica-encapsulated gold nanorods for chemo-photothermal therapy with near-infrared radiation. *Biomaterials* **2013**, *34*, 3150−3158.
(35) Zhang, Q.; Wang, L.; Jiang, Y.; Gao, W.; Wang, Y.; Yang, X.; Yang, X.; Liu, Z. Gold nanorods with silica shell and PAMAM dendrimers for efficient photothermal therapy and low toxic codelivery of anticancer drug and siRNA. *Adv. Mater. Interfaces* **2017**, *4*, 1701166.
(36) Liu, Y.; Xu, M.; Chen, Q.; Guan, G.; Hu, W.; Zhao, X.; Qiao, M.; Hu, H.; Liang, Y.; Zhu, H.; Chen, D. Gold nanorods/mesoporous silica-based nanocomposite as theranostic agents for targeting near-infrared imaging and photothermal therapy induced with laser. *Int. J. Nanomed.* **2015**, *10*, 4747−4761.
(37) Wilschefski, S. C.; Baxter, M. R. Inductively coupled plasma mass spectrometry: introduction to analytical aspects. *Clin. Biochem. Rev.* **2019**, *40*, 115−133.
(38) Elzey, S.; Tsai, D.-H.; Rabb, S. A.; Yu, L. L.; Winchester, M. R.; Hackley, V. A. Quantification of ligand packing density on gold nanoparticles using ICP-OES. *Anal. Bioanal. Chem.* **2012**, *403*, 145−149.
(39) Peñaloza, J. P.; Márquez-Miranda, V.; Cabaña-Brunod, M.; Reyes-Ramírez, R.; Llancalahuen, F. M.; Vilos, C.; Maldonado-Biermann, F.; Velásquez, L. A.; Fuentes, J. A.; González-Nilo, F. D.; Rodríguez-Díaz, M.; Otero, C. Intracellular trafficking and cellular uptake mechanism of PHBV nanoparticles for targeted delivery in epithelial cell lines. *J. Nanobiotechnol.* **2017**, *15*, 1−15.
(40) Decher, G.; Hong, J. D.; Schmitt, J. Buildup of ultrathin multilayer films by a self-assembly process: III. Consecutively alternating adsorption of anionic and cationic polyelectrolytes on charged surfaces. *Thin Solid Films* **1992**, *210−211*, 831−835.
(41) Shiotani, A.; Akiyama, Y.; Kawano, T.; Niidome, Y.; Mori, T.; Katayama, Y.; Niidome, T. Active accumulation of gold nanorods in tumor in response to near-infrared laser irradiation. *Bioconjugate Chem.* **2010**, *21*, 2049−2054.
(42) Gordel, M.; Piela, K.; Kołkowski, R.; Koźlecki, T.; Buckle, M.; Samoć, M. End-to-end self-assembly of gold nanorods in isopropanol solution: experimental and theoretical studies. *J. Nanopart. Res.* **2015**, *17*, 477.
(43) Fujiwara, Y.; Hizukuri, Y.; Yamashiro, K.; Makita, N.; Ohnishi, K.; Takeya, M.; Komohara, Y.; Hayashi, Y. Guanylate-binding protein 5 is a marker of interferon-γ-induced classically activated macrophages. *Clin. Transl. Immunol.* **2016**, *5*, No. e111.
(44) Nakase, I.; Takeuchi, T.; Tanaka, G.; Futaki, S. Methodological and cellular aspects that govern the internalization mechanisms of arginine-rich cell-penetrating peptides. *Adv. Drug Delivery Rev.* **2008**, *60*, 598−607.
(45) Kocherova, I.; Bryja, A.; Mozdziak, P.; Angelova Volponi, A.; Dyszkiewicz-Konwińska, M.; Piotrowska-Kempisty, H.; Antosik, P.; Bukowska, D.; Bruska, M.; Iżycki, D.; Zabel, M.; Nowicki, M.; Kempisty, B. Human umbilical vein endothelial cells (HUVECs) co-culture with osteogenic cells: From molecular communication to engineering prevascularised bone grafts. *J. Clin. Med.* **2019**, *8*, 1602.
(46) Ginhoux, F.; Guilliams, M. Tissue-resident macrophage ontogeny and homeostasis. *Immunity* **2016**, *44*, 439−449.
(47) Ishii, H.; Shirai, T.; Makino, C.; Nishikata, T. Mitochondrial inhibitor sodium azide inhibits the reorganization of mitochondria-rich cytoplasm and the establishment of the anteroposterior axis in ascidian embryo. *Dev., Growth Differ.* **2014**, *56*, 175−188.
(48) Manzanares, D.; Ceña, V. Endocytosis: The nanoparticle and submicron nanocompounds gateway into the cell. *Pharmaceutics* **2020**, *12*, 371.
(49) Koivusalo, M.; Welch, C.; Hayashi, H.; Scott, C. C.; Kim, M.; Alexander, T.; Touret, N.; Hahn, K. M.; Grinstein, S. Amiloride inhibits macropinocytosis by lowering submembranous pH and preventing Rac1 and Cdc42 signaling. *J. Cell Biol.* **2010**, *188*, 547−563.
(50) Dutta, D.; Donaldson, J. G. Search for inhibitors of endocytosis: Intended specificity and unintended consequences. *Cell. Logist.* **2012**, *2*, 203−208.
(51) Vercauteren, D.; Vandenbroucke, R. E.; Jones, A. T.; Rejman, J.; Demeester, J.; De Smedt, S. C.; Sanders, N. N.; Braeckmans, K. The use of inhibitors to study endocytic pathways of gene carriers: optimization and pitfalls. *Mol. Ther.* **2010**, *18*, 561−569.
(52) Wilhelm, L. P.; Voilquin, L.; Kobayashi, T.; Tomasetto, C.; Alpy, F. Intracellular and plasma membrane cholesterol labeling and quantification using filipin and GFP-D4. *Methods Mol. Biol.* **2019**, *1949*, 137−152.
(53) Cheng, J. P. X.; Mendoza-Topaz, C.; Howard, G.; Chadwick, J.; Shvets, E.; Cowburn, A. S.; Dunmore, B. J.; Crosby, A.; Morrell, N. W.; Nichols, B. J. Caveolae protect endothelial cells from membrane rupture during increased cardiac output. *J. Cell Biol.* **2015**, *211*, 53−61.
(54) Frank, P. G.; Woodman, S. E.; Park, D. S.; Lisanti, M. P. Caveolin, caveolae, and endothelial cell function. *Arterioscler., Thromb., Vasc. Biol.* **2003**, *23*, 1161−1168.
(55) Tanaka, G.; Nakase, I.; Fukuda, Y.; Masuda, R.; Oishi, S.; Shimura, K.; Kawaguchi, Y.; Takatani-Nakase, T.; Langel, Ü.; Gräslund, A.; Okawa, K.; Matsuoka, M.; Fujii, N.; Hatanaka, Y.; Futaki, S. CXCR4 stimulates macropinocytosis: implications for cellular uptake of arginine-rich cell-penetrating peptides and HIV. *Chem. Biol.* **2012**, *19*, 1437−1446.
(56) Zhang, M.; Chen, X.; Li, C.; Shen, X. Charge-reversal nanocarriers: An emerging paradigm for smart cancer T nanomedicine. *J. Controlled Release* **2020**, *319*, 46−62.
(57) Niidome, T.; Akiyama, Y.; Shimoda, K.; Kawano, T.; Mori, T.; Katayama, Y.; Niidome, Y. In Vivo Monitoring of Intravenously Injected Gold Nanorods Using Near-Infrared Light. *Small* **2008**, *4*, 1001−1007.
(58) Gole, A.; Murphy, C. J. Polyelectrolyte-coated gold nanorods: synthesis, characterization and immobilization. *Chem. Mater.* **2005**, *17*, 1325−1330.
(59) Wan, J.; Wang, J.-H.; Liu, T.; Xie, Z.; Yu, X.-F.; Li, W. Surface chemistry but not aspect ratio mediates the biological toxicity of gold nanorods in vitro and in vivo. *Sci. Rep.* **2015**, *5*, 11398.

https://dx.doi.org/10.1021/acsomega.0c05162
ACS Omega 2020, 5, 32744−32752

(60) Cifuentes-Rius, A.; Ivask, A.; Das, S.; Penya-Auladell, N.; Fabregas, L.; Fletcher, N. L.; Houston, Z. H.; Thurecht, K. J.; Voelcker, N. H. Gold nanocluster-mediated cellular death under electromagnetic radiation. *ACS Appl. Mater. Interfaces* **2017**, *9*, 41159−41167.
(61) Uddin, J.; Rahman, A.; Ghann, W.; Kang, H.; Rahman, A. K. Terahertz multispectral imaging for the analysis of gold nanoparticles' size and the number of unit cells in comparison with other techniques. *Int. j. biosens. bioelectron.* **2018**, *4*, 169.

https://dx.doi.org/10.1021/acsomega.0c05162
ACS Omega 2020, 5, 32744−32752